

ORIGINAL ARTICLE

Impact of attenuation correction on segmental score analysis of myocardial perfusion imaging

Lubna K Jadoon, Hasan Raza*, Minhaj Maqbool, Bashir Ahmed, Sumaira Mushtaq, Aniq Jabeen, Muhammad A Memon

Nuclear Medicine Department, Atomic Energy Medical Centre, Jinnah Postgraduate Medical Centre (JPMC), Karachi

Abstract

Aims To assess the impact of attenuation correction in reducing artifacts and the influence of gender and body mass on the effect of attenuation correction.

Methods 102 patients referred for myocardial perfusion imaging (mean age: 53.24 ± 12.7) were enrolled. They all underwent stress (dynamic or pharmaceutical) and rest Tc-99m MIBI studies. Polar maps of the left ventricular cavity with 17 segments of both the non-corrected (NC) and attenuation corrected (AC) images were generated and semi-quantitatively analyzed by software automatically.

Results Segmental scores in inferior wall were significantly low ($p < 0.05$) particularly in male population irrespective of BMI. AC didn't do significant impact in score values in anterior wall of female population ($p > 0.05$). AC also generated artifactual perfusion defects in apex and apical segments ($p < 0.05$).

Conclusion This study demonstrates that Attenuation correction using hybrid SPECT-CT improved average myocardial perfusion uptake in inferior regions and this technique is more beneficial to male populace.

Key words: Attenuation correction, myocardial perfusion imaging, Tc-99m MIBI

Introduction

Attenuation is a major source of inaccuracies for Single Photon Emission Computed Tomography (SPECT) myocardial imaging studies. It alters the absolute and relative measurements of pharmaceutical uptake, distorts the shape of the ventricle, and dominates all other competing artifacts (partial volume, photon scatter, and cardiac motion, etc.) causing an increase in false-positive studies, by simulating real defects resulting the decrement in specificity of perfusion imaging [2].

Soft-tissue attenuation is the loss of photons as they pass through a medium (e.g. soft tissue) either due to photoelectric effect or Compton scatter is called attenuation. The percentage of photons lost depends on the energy of the photons, the density of the material and the thickness of the material [2].

New hardware and software are continually being developed to create patient-specific

*Correspondence

Dr. Hasan Raza
Atomic Energy Medical Centre (AEMC)
Jinnah Postgraduate Medical Centre
Rafique Shaheed Road, Karachi
Email: hrnoor@hotmail.com
Tel: +9221 9205693-4
Fax: +9221 99201354

non-uniform attenuation maps in order to permit attenuation correction (AC) during reconstruction of SPECT images [3, 4]. Many of them based on transmission scanning with external radioactive or X-ray sources. In our Institute, Computer Tomography (CT) based, attenuation correction is being done using Hybrid SPECT-CT system (Hawkeye) for myocardial perfusion imaging as a routine procedure to increase the specificity of results.

In the current study, we evaluated the impact of attenuation correction in reducing artifacts and the influence of gender and body mass on the effect of attenuation correction.

Materials and Methods

We studied a group of 102 patients 66 males and 36 females who had been referred to our department with diagnostic as well as risk stratification purposes as part of their clinical management. Patients with MI, LBBB, history of revascularization or cardiomyopathies were excluded from the study.

Image acquisition and processing

All patients underwent stress and rest studies with a four-hour gap in between as one-day protocol for which they were injected Tc-99m Methoxy-isobutyl-isonitrile (MIBI) 10 & 30 mCi respectively, according to standard protocol. Either the patients were exercised on the treadmill ($n = 65$) or underwent pharmacological (Dipyridamole) ($n = 37$) stress. The Hybrid GE Infinia Hawkeye dual-head gamma camera equipped with low-energy high-resolution collimators and low-resolution CT were used.

Acquisition was performed, on average, 30-60 minutes postinjection. A total of 64 projections (40 s/projection) were obtained using a 64x64 matrix with a starting angle of 45 degrees right anterior oblique (RAO) position to the 135 degrees left posterior oblique position. A 20% symmetric energy window centered at 140 keV was used. A zoom of 1.33 was applied during acquisition. The transmission study was done at the end of study, without changing the position of the patient.

The reconstruction was performed using a Butterworth filter and the filtered back-projection method on processing computer. Before reconstruction, the projection data were reviewed in cine mode to rule out the possibility of patient motion.

Data Analysis

All the studies were assessed for any mal-registration and patient movement. If there was slight misregistration between emission and transmission data, the images were reprocessed but discarded if there was evidence of significant patient motion or misregistration during acquisition.

The Emory Computed Tomography (ECT) software, generated polar maps and then automatically graded the 17 segments for perfusion defects. The segments were graded for the severity of perfusion defects using a 5-point scoring system (0, definitely normal; 1, mild reduction of radioisotope uptake; 2, moderate reduction of radioisotope uptake; 3, severe reduction of radioisotope uptake; 4, absence of detectable tracer uptake) [5]. Segmental scores for stress (SS) and rest (RS) were automatically generated. The difference score (DS) was also computed as the difference between SS and RS and is a measure of perfusion defect reversibility reflecting inducible ischaemia (Figure 1). Mean SS, RS and DS scores \pm standard deviation (SD) of all segments of both image sets i.e. Non-corrected and Attenuation corrected (NC & AC) were then compared using student paired t test.

Results

In this prospective study, data of 11 patients (4 females and 7 males) were discarded due to severe motion artifacts and/or mis registration between CT and SPECT images. There were 91 patients; their mean age was 53.24 ± 12.7 years, with a range of 30-78 years and mean height was 162.0 ± 25.18 cm. The study population had mean weight of 72.70 ± 15.56 kg. Characteristic of study population are shown in Table 1.

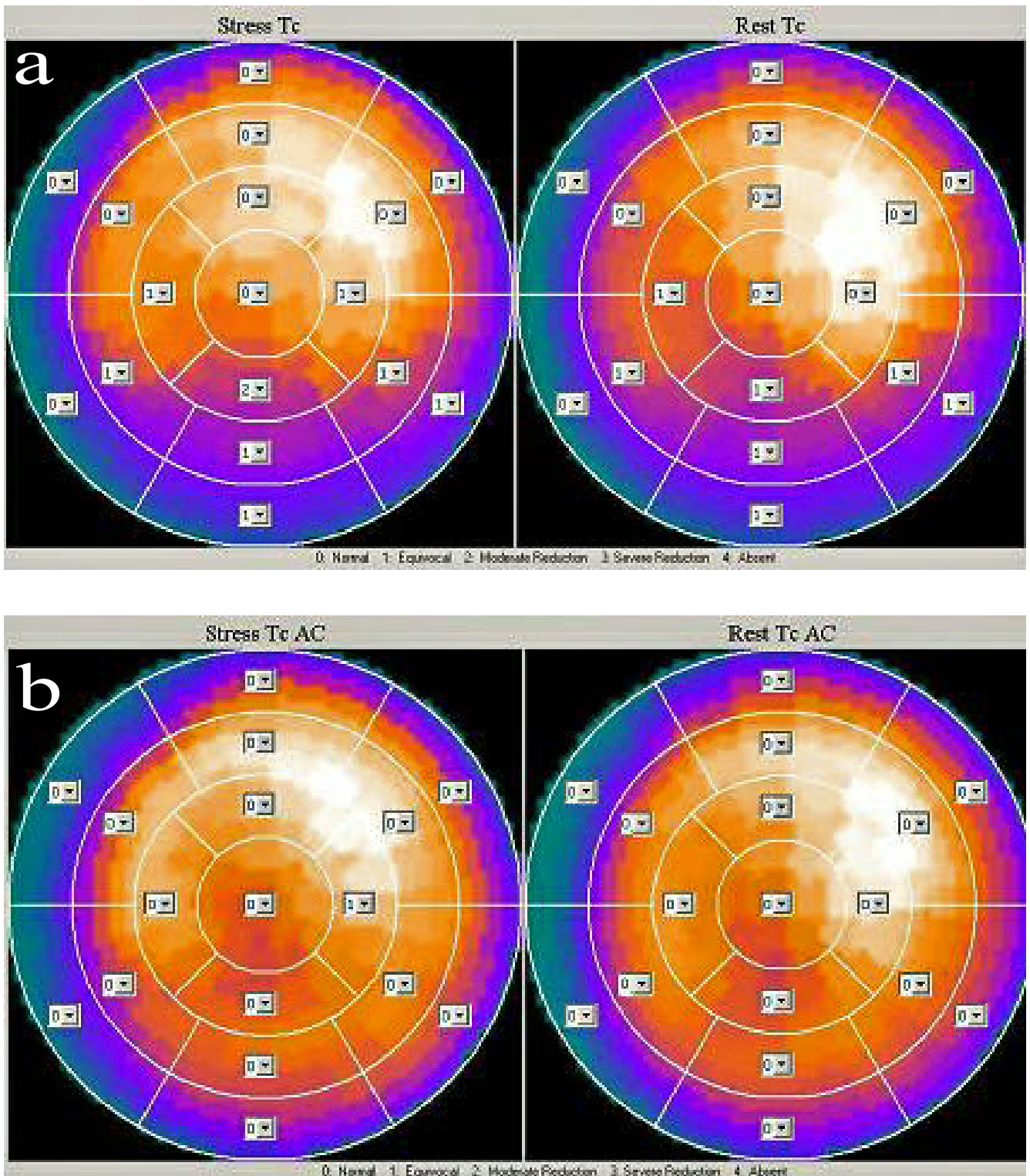


Figure 1 Comparison of the segmental scores on polar maps for NC and AC. The NC images reveal fixed perfusion defects in inferior, infero-septal and infero-lateral walls (a). The defects improved by attenuation correction (b)

Table 1 Demographics of the study population

	Population
n	91
Age	53.24±12.7
BMI (mean ± SD)	27.18 ±6.2
Female	32 (35%)
Male	59 (65%)
Hypertension	55 (60%)
Diabetes	23 (25%)
Family History	29 (32%)
Hyperlipidemia	17 (18%)
Smoking	28 (19%)
Abnormal BMI	58 (64%)

Semi-Quantitative Results

Semi-quantitative MPS analyses for all patients found decrease in score values upon attenuation correction in most of the segments. There was more marked improvement in mid inferior and basal inferior segments. However, significant increase in stress and rest scores of apex and apical regions were also noted. In contrast to the inferior and anterior walls, the lateral wall showed no significant change with attenuation correction (Table 2).

For the male study population, the mean stress, rest and difference scores show significant increase in tracer uptake i.e. reduction of scores in mid inferior and basal inferior segments upon attenuation correction, a clear tendency to reduce score values with attenuation correction, signifying the presence of inferior wall attenuation artifacts in the male population. A non significant improvement in uptake was also noted in some other segments like in basal anterior, basal anterolateral, basal inferolateral, mid inferolateral segments. A decrease in tracer uptake was observed in apex, apical lateral and apical anterior segments (Table 3).

For the female study population, the comparison of NC and AC semi quantitative collective data showed similar trend in apex and apical segments i.e. increase in score values after attenuation correction. Appreciable but insignificant reduction in score values was noted in the anterior and anterolateral wall segments. Non-significant reduction of defects size was also noted in basal inferior and mid inferior segments (Table 4).

For the normal weight population, the stress, rest and difference scores showed appreciable decrease in score values in the inferior wall segments upon attenuation correction but with a non significant p value. Rest of the segments showed similar changes in score values upon attenuation correction as of previous groups (Table 5).

For the overweight population, the automatically generated semi quantitative scores showed increase uptake in the mid inferior basal inferior and mid inferolateral segments as a result of attenuation correction but this betterment in uptake of radiotracer was insignificant (Table 6).

Table 2 Overall segmental average and standard deviation values of stress, rest and difference scores on the polar maps with NC and AC

Segment	SS-NC	SS-AC	p	RS-NC	RS-AC	p	DS-NC	DS-AC	p
Apex	0.74±1.22	1.41±1.30	0	0.35±0.89	0.96±1.18	0	0.46±0.97	0.59±0.94	0.46
B-antsep	0.03±0.18	0	0.08	0	0	0	0.04±0.19	0	0.15
B-ant	0.13±0.40	0.07±0.25	0.20	0	0.03±0.22	0.32	0.15±0.42	0.03±0.22	0.05
M-ant	0.46±0.89	0.52±0.93	0.70	0.21±0.60	0.31±0.74	0.72	0.30±0.62	0.25±0.63	0.60
M-antsept	0.54±0.85	0.68±1.01	0.33	0.24±0.64	0.56±0.93	0.02	0.35±0.67	0.19±0.65	0.12
B-antlat	0.10±0.40	0.1±0.43	1.00	0.03±0.16	0.09±0.43	0.22	0.09±0.40	0.03±0.42	0.43
B-inflat	0.27±0.73	0.19±0.60	0.40	0.11±0.52	0.06±0.29	0.58	0.19±0.53	0.11±0.55	0.76
M-antlat	0.51±0.85	0.69±0.79	0.17	0.25±0.62	0.48±0.83	0.06	0.31±0.66	0.23±0.80	0.46
M-inflat	0.59±0.92	0.52±0.86	0.56	0.42±0.89	0.35±0.69	0.92	0.23±0.63	0.20±0.62	0.59
Api-ant	0.55±1.10	0.96±1.15	0.02	0.28±0.78	0.58±0.96	0.09	0.32±0.70	0.42±0.66	0.45
Api-sept	0.62±1.05	0.84±1.13	0.19	0.38±0.91	0.65±1.01	0.05	0.33±0.87	0.29±0.78	0.63
Api-lat	0.68±0.95	1.17±1.01	0	0.30±0.69	0.68±0.92	0	0.46±0.65	0.55±0.88	0.47
B-infsept	0.08±0.45	0.02±0.21	0.30	0.04±0.34	0	0.32	0.05±0.22	0.03±0.23	0.70
B-inf	0.32±0.87	0.04±0.30	0	0.16±0.60	0	0.04	0.18±0.53	0.05±0.32	0.22
M-infsept	0.48±0.90	0.37±0.79	0.29	0.26±0.67	0.31±0.67	0.45	0.25±0.80	0.08±0.68	0.10
M-inf	0.84±1.14	0.37±0.76	0	0.44±0.88	0.13±0.44	0.04	0.45±0.73	0.24±0.56	0.06
Api-inf	0.67±0.94	0.77±0.84	0.51	0.41±0.76	0.5±0.82	0.36	0.31±0.56	0.37±0.76	0.56

For the obese population, no significant change in the score values is noted on attenuation correction. It is deduced from the semi quantitative analysis, that there is no significant improvement in tracer uptake in the study population on the basis of body mass index (Table 7).

Discussion

Initially, attenuation correction in areas of non-homogenous attenuation such as chest was achieved by radionuclide-based transmission images, but CT-based attenuation correction is rapidly emerging as the standard for SPECT [4]. The transition from radionuclide transmission source to CT for attenuation correction is

due to the added benefits of less noise, faster acquisition, no influence of the SPECT radionuclide on CT data and no need to replace decayed transmission source [6]. Masood *et al.* first validated the clinical efficacy of CT-based AC of MPI and found proof that it did indeed improve the diagnostic accuracy of the MPI SPECT [7].

In our study, we tried to assess the impact of CT-based attenuation correction on myocardial perfusion scintigraphy. We studied patients' scans semi-quantitatively. By semi-quantitative analysis, we just wanted to observe the outcome on the uptake/count pattern and/or homogeneity of the left ventricle after attenuation correction and the influence of gender and body mass on the effect of attenuation correction.

Table 3 Segmental average and standard deviation values of stress, rest and difference scores in the male population with *p* values derived from the polar maps with NC and AC

Segment	SS-NC	SS-AC	<i>p</i>	RS-NC	RS-AC	<i>p</i>	DS-NC	DS-AC	<i>p</i>
Apex	0.87±1.26	1.62±1.33	0	0.4±1.01	1.15±1.19	0	0.55±0.96	0.59±0.89	0.68
B-antsep	0.05±0.22	0	0.08	0	0	0	0.06±0.23	0	0.08
B-ant	0.05±0.22	0.03±0.18	0.65	0	0	0	0.06±0.23	0.04±0.19	0.32
M-ant	0.32±0.75	0.55±0.93	0.15	0.18±0.55	0.35±0.75	0.21	0.16±0.42	0.25±0.67	0.60
M-antsept	0.47±0.81	0.83±1.03	0.03	0.31±0.72	0.71±0.99	0.03	0.2±0.56	0.18±0.72	0.88
B-antlat	0.13±0.47	0.08±0.33	0.51	0.04±0.19	0.04±0.27	1.00	0.11±0.46	0.06±0.45	0.65
B-inflat	0.35±0.84	0.22±0.61	0.34	0.13±0.58	0.06±0.30	0.53	0.24±0.61	0.19±0.62	1.00
M-antlat	0.38±0.87	0.62±0.8	0.17	0.22±0.60	0.5±0.81	0.10	0.20±0.49	0.16±0.65	0.86
M-inflat	0.6±1.01	0.47±0.93	0.49	0.44±0.88	0.33±0.70	0.61	0.22±0.53	0.18±0.61	0.73
Api-ant	0.48±1.10	1.07±1.21	0.01	0.33±0.84	0.73±1.00	0.02	0.2±0.52	0.41±0.65	0.15
Api-sept	0.57±1.05	0.92±1.18	0.11	0.48±1.04	0.82±1.06	0.16	0.15±0.68	0.18±0.75	0
Api-lat	0.73±1.02	1.35±1.01	0	0.38±0.78	0.79±0.90	0	0.43±0.60	0.63±0.77	0.16
B-infsept	0.12±0.56	0.03±0.26	0.30	0.06±0.41	0	0.32	0.07±0.26	0.04±0.27	0.71
B-inf	0.42±1.03	0.07±0.36	0.01	0.22±0.72	0	0.05	0.24±0.58	0.07±0.38	0.28
M-infsept	0.52±0.89	0.43±0.77	0.58	0.39±0.79	0.44±0.77	0.49	0.13±0.67	0	0.16
M-inf	0.87±1.26	0.32±0.72	0	0.56±1.02	0.17±0.50	0.06	0.35±0.62	0.19±0.44	0.13
Api-inf	0.75±1.02	0.82±0.87	0.72	0.46±0.84	0.57±0.77	0.633	0.35±0.59	0.37±0.65	0.74

Our study revealed considerable reductions in score values (i.e. increase in tracer uptake) in basal and mid inferior segments while insignificant reduction was also observed in other regions. Another prominent thing that was observed in semi quantitative analysis was a significant increase in score values of apex and the apico-anterior wall and an insignificant increase in antero-septal and apical lateral walls.

It has long been recognized that attenuation correction may create artifactual defects in apex and adjacent anterior segments, by over-correction [8]. The apical thinning is a well-known phenomenon when using the x-ray

based AC method [9]. This phenomenon has been extensively studied by Fricke *et al.* [10] using both patients and phantoms on the GE Hawkeye system. They found apical or anterior perfusion defects in the attenuation corrected (AC) scans in 27 of 140 patients (19%) who had a normal non-AC scan.

Most of the researchers believe that effect in the inferior wall is the actual removal of an attenuation artifact as it corresponds better with clinical opinion. While creation or enhancement of defect in apex and anterior walls are artifactual, as they usually do not correspond with clinical opinion [11].

Table 4 Segmental average and standard deviation values of stress, rest and difference scores in the female population with *p* value derived from the polar maps with NC and AC

Segment	SS-NC	SS-AC	<i>p</i>	RS-NC	RS-AC	<i>p</i>	DS-NC	DS-AC	<i>p</i>
Apex	0.48±1.12	1±1.14	0.01	0.25±0.58	0.56±1.08	0.14	0.30±0.99	0.6±1.04	0.24
B-antsep	0	0	0	0	0	0	0	0	0
B-ant	0.29±0.59	0.13±0.35	0.20	0	0.08±0.40	0.32	0.33±0.62	0	0.00
M-ant	0.74±1.06	0.47±0.94	0.08	0.26±0.71	0.24±0.72	0.71	0.59±0.84	0.24±0.52	0.02
M-antsept	0.68±0.91	0.37±0.93	0.09	0.11±0.42	0.23±0.71	0.18	0.67±0.78	0.2±0.50	0.00
B-antlat	0.03±0.18	0.13±0.57	0.32	0	0.2±0.65	0.13	0.04±0.20	-0.04	0.16
B-inflat	0.13±0.43	0.13±0.57	1.00	0.07±0.38	0.08±0.28	1.00	0.07±0.27	-0.04	0.16
M-antlat	0.74±0.77	0.83±0.75	0.32	0.30±0.67	0.43±0.88	0.35	0.52±0.89	0.36±1.03	0.40
M-inflat	0.58±0.72	0.63±0.72	0.57	0.39±0.92	0.41±0.69	1.00	0.25±0.80	0.22±0.64	1.000
Api-ant	0.68±1.11	0.73±1.01	0.65	0.19±0.63	0.26±0.81	0.32	0.58±0.95	0.44±0.70	0.46
Api-sept	0.71±1.07	0.7±1.02	0.88	0.15±0.46	0.31±0.84	0.35	0.72±1.10	0.52±0.82	0.42
Api-lat	0.58±0.81	0.8±0.92	0.20	0.15±0.46	0.44±0.93	0.10	0.52±0.75	0.37±1.08	0.28
B-infsept	0	0	0	0	0	0	0	0	0
B-inf	0.13±0.34	0	0.08	0.04±0.20	0	0.32	0.04±0.35	0	1.00
M-infsept	0.42±0.92	0.23±0.82	0.18	0	0	0	0.5±0.99	0.29±0.91	0.26
M-inf	0.77±0.88	0.47±0.82	0.16	0.19±0.40	0.04±0.20	0.04	0.65±0.89	0.38±0.77	0.34
Api-inf	0.52±0.77	0.67±0.76	0.32	0.31±0.55	0.33±0.92	1.00	0.23±0.51	0.38±0.97	0.40

Matsunari *et al.* [12] showed that in phantoms and patients with a low likelihood of CAD, attenuation correction produced an increase in the count density in the inferior wall due to photon scatter from extracardiac activity and a relative decrease in the count density in myocardial segments other than the inferior wall due to the effect of normalization of the counts to the region showing greatest activity. Savi *et al.* [13] suggested that the decrease in anterior wall activity resulted from the relative overestimation of inferior wall uptake rather than the underestimation of anterior wall uptake. In other words, the presence of sub diaphragmatic activity may result in both an increase in uptake in the inferior wall and

a decrease in uptake in the anterior wall [14], rather than in the normal tissues [4].

Our results divulged significant improvement in inferior wall segments in male gender while no significant change was observed in any segment in female populace. Another notable thing is that the anterior wall segments did not show any significant difference between the genders. This is in contrast to our expectations. Nakajima *et al.* reported that the difference on myocardial perfusion upon attenuation correction in the two genders was significant in the mid and apical inferior segments, showing lower values in males. Moreover, there were insignificant differences

Table 5 Segmental average and standard deviation values of stress, rest and difference scores in the non obese population with *p* value derived from the polar maps with NC and AC

Segment	SS-NC	SS-AC	<i>p</i>	RS-NC	RS-AC	<i>p</i>	DS-NC	DS-AC	<i>p</i>
Apex	0.97±1.36	1.69±1.42	0.01	0.43±1.17	1.07±1.30	0	0.68±1.06	0.79±0.98	0.75
B-antsep	0.09±0.30	0.09±0	0	0	0	0	0.11±0.31	0.11±0	0
B-ant	0.16±0.37	0.06±0.25	0.18	0	0	0	0.18±0.39	0	0.18
M-ant	0.34±0.70	0.59±0.87	0.76	0.29±0.66	0.57±0.92	1.0	0.11±0.31	0.04±0.58	0.81
M-antsept	0.31±0.69	0.75±1.02	0.89	0.32±0.67	0.66±0.97	0.13	0.04±0.19	0.17±0.93	0.08
B-antlat	0.16±0.51	0.09±0.30	0.64	0	0.07±0.38	0.77	0.18±0.55	0.04±0.51	0.71
B-inflat	0.31±0.69	0.16±0.45	1.00	0.04±0.19	0.04±0.19	0.66	0.32±0.67	0.14±0.52	0.50
M-antlat	0.38±0.83	0.81±0.86	0.75	0.18±0.55	0.59±0.87	1.00	0.25±0.52	0.24±0.74	1.00
M-inflat	0.59±0.98	0.59±1.07	0.80	0.43±0.88	0.39±0.83	0.64	0.25±0.52	0.21±0.74	0.35
Api-ant	0.56±1.13	1.31±1.33	0.38	0.43±0.96	0.83±1.00	0.36	0.21±0.57	0.62±0.78	0.77
Api-sept	0.59±1.07	1.0±1.27	0.55	0.57±1.10	0.83±1.17	0.11	0.11±0.74	0.28±0.80	0.86
Api-lat	0.72±1.08	1.41±1.07	0.11	0.36±0.87	0.72±0.96	0.03	0.46±0.51	0.76±0.79	0.32
B-infsept	0.22±0.75	0.06±0.35	0	0.11±0.57	0	0	0.14±0.36	0.07±0.38	0
B-inf	0.44±1.11	0.06±0.35	0.16	0.21±0.63	0	0.32	0.29±0.66	0.07±0.38	1.0
M-infsept	0.47±1.02	0.34±0.83	0.71	0.5±0.92	0.43±0.69	0.42	0.04±0.51	-0.04	0.46
M-inf	0.94±1.41	0.42±0.88	0.11	0.62±1.16	0.17±0.61	0.26	0.45±0.63	0.21±0.42	0.62
Api-inf	0.84±1.11	0.88±0.91	0.22	0.57±0.96	0.68±0.94	0.49	0.39±0.50	0.29±0.60	0.32

in the anterior segments between genders [15]. Okuda *et al.* believed this is due to relatively more homogenous body habitus of their populace (Eastern Asian males and females) as compared to European and American populations [9]. The same could be reason in our populations. However, many studies had proved that breast attenuation does cause artifacts in the anterior and anterolateral segments [16, 17]. Our study proved that effect of attenuation correction is same in all the three groups classified according to BMI, thus, reinforcing the fact that inferior wall attenuation artifacts are related to the diaphragmatic position rather

than the body size. Our results are also in agreement with observations reported by Biedermann *et al.* [18] who investigated the relationship between BMI and attenuation effects using SPECT in patients.

This study has some limitations. First, no scatter correction was used; additional scatter subtraction in combination with attenuation correction might further improve the results. Second, the body contours were obtained from CT mapping and information of breast tissues was not precisely traced. The effect of dense breasts overlying the anterior wall should be evaluated in further studies.

Table 6 Segmental average and standard deviation values of stress, rest and difference scores in the overweight population with *p* value derived from the polar maps with NC and AC

Segment	SS-NC	SS-AC	<i>p</i>	RS-NC	RS-AC	<i>p</i>	DS-NC	DS-AC	<i>p</i>
Apex	0.62±1.15	1.41±1.24	0.01	0.32±0.77	1.12±1.24	0.00	0.33±0.62	0.44±0.89	0.75
B-antsep	0	0	0	0	0	0	0	0	0
B-ant	0.10±0.41	0	0.18	0	0	0	0.11±0.42	0	0.18
M-ant	0.55±0.99	0.48±1.02	0.76	0.22±0.58	0.15±0.54	1.00	0.37±0.69	0.38±0.70	0.81
M-antsept	0.72±0.96	0.69±0.97	0.89	0.30±0.79	0.59±1.01	0.13	0.48±0.75	0.15±0.37	0.08
B-antlat	0.10±0.41	0.10±0.66	0.64	0.08±0.27	0.08±0.59	0.77	0.04±0.34	0.04±0.39	0.71
B-inflat	0.38±0.98	0.38±0.90	1.00	0.19±0.79	0.08±0.39	0.66	0.19±0.56	0.23±0.71	0.50
M-antlat	0.66±0.94	0.72±0.75	0.75	0.37±0.69	0.5±0.79	1.00	0.30±0.54	0.21±0.69	1.00
M-inflat	0.72±1.03	0.66±0.81	0.80	0.57±0.92	0.43±0.63	0.64	0.18±0.61	0.25±0.52	0.35
Api-ant	0.59±1.12	0.79±1.01	0.38	0.31±0.74	0.59±1.01	0.36	0.31±0.62	0.22±0.42	0.77
Api-sept	0.72±1.13	0.90±1.11	0.55	0.38±0.98	0.81±1.06	0.11	0.42±0.86	0.19±0.85	0.86
Api-lat	0.69±0.93	1.07±1.00	0.11	0.41±0.69	0.96±1.02	0.03	0.37±0.63	0.19±0.79	0.32
B-infsept	0	0	0	0	0	0	0	0	0
B-inf	0.34±0.94	0.07±0.37	0.16	0.19±0.79	0	0.32	0.15±0.46	0.08±0.39	1.00
M-infsept	0.62±0.94	0.55±0.95	0.71	0.22±0.58	0.38±0.80	0.42	0.41±1.05	0.19±0.98	0.46
M-inf	0.86±1.09	0.45±0.78	0.11	0.44±0.85	0.19±0.490	0.26	0.41±0.80	0.31±0.68	0.62
Api-inf	0.62±0.86	0.86±0.79	0.22	0.37±0.69	0.54±0.86	0.49	0.30±0.61	0.42±0.99	0.32

Conclusions

Our study validated that CT based attenuation correction significantly reduces defect scores in the inferior segment. The reduction in defect score is more evident in men than in women irrespective of their BMI. In the anterior segment the effects of attenuation correction are not remarkable. Furthermore, this technique is prone to develop artifacts in apex and apical regions. It is therefore pertinent to study the NC and AC images simultaneously.

References

1. Garcia EV. SPECT attenuation correction: an essential tool to realize nuclear cardiology's manifest destiny. *J Nucl Cardiol* 2007; 14:16-24.
2. Wilson M, Bianco JA, Tu RK, Zager LV. section 3: Fundamentals of nuclear medicine. Radiation detection. In Wilson M (eds), *Text book of nuclear medicine*. Philadelphia: Lippincott-Raven 1998; 415-436.

Table 7 Segmental average and standard deviation values of stress, rest and difference scores in the obese population with *p* value derived from the polar maps with NC and AC

Segment	SS-NC	SS-AC	<i>p</i>	RS-NC	RS-AC	<i>p</i>	DS-NC	DS-AC	<i>p</i>
Apex	0.60	1.10	0.01	0.30	0.69	0	0.37	0.52	0.75
B-antsep	0	0	0	0	0	0	0	0	0
B-ant	0.13±0.43	0.14±0.35	0.18	0	0.08±0.39	0	0.15±0.46	0.08±0.39	0.18
M-ant	0.5±0.97	0.48±0.91	0.76	0.11±0.58	0.19±0.63	1.00	0.44±0.75	0.35±0.56	0.81
M-antsept	0.6±0.86	0.59±1.09	0.89	0.11±0.42	0.42±0.81	0.13	0.56±0.80	0.23±0.51	0.08
B-antlat	0.03±0.18	0.03±0.19	0.64	0±0	0.08±0.28	0.77	0.04±0.20	-0.04	0.71
B-inflat	0.13±0.43	0.03±0.19	1.00	0.12±0.43	0.08±0.28	0.66	0.04±0.20	-0.04	0.50
M-antlat	0.5±0.78	0.52±0.74	0.75	0.19±0.63	0.33±0.83	1.00	0.38±0.90	0.22±0.97	1.00
M-inflat	0.47±0.73	0.31±0.60	0.80	0.26±0.86	0.23±0.59	0.64	0.26±0.76	0.12±0.59	0.35
Api-ant	0.5±1.07	0.72±1.00	0.38	0.11±0.58	0.30±0.82	0.36	0.44±0.89	0.41±0.69	0.77
Api-sept	0.53±0.97	0.62±0.98	0.55	0.15±0.46	0.31±0.68	0.11	0.48±1.00	0.4±0.71	0.86
Api-lat	0.63±0.85	1±0.93	0.11	0.14±0.45	0.36±0.68	0.03	0.54±0.79	0.68±0.98	0.32
B-infsept	0	0	0	0	0	0	0	0	0
B-inf	0.17±0.38	0	0.16	0.08±0.28	0	0.32	0.08±0.40	0	1.00
M-infsept	0.37±0.72	0.21±0.49	0.71	0.04±0.20	0.08±0.41	0.42	0.32±0.75	0.08±0.28	0.46
M-inf	0.7±0.84	0.21±0.56	0.11	0.2±0.41	0	0.26	0.52±0.77	0.21±0.59	0.62
Api-inf	0.53±0.82	0.55±0.78	0.22	0.28±0.54	0.25±0.53	0.49	0.24±0.60	0.42±0.65	0.32

- Links JM, DePuey EG, Taillefer R, Becker LC. Attenuation correction and gating synergistically improve the diagnostic accuracy of myocardial perfusion SPECT. *J Nucl Cardiol* 2002; 9:183-187.
- Zaidi H, Hasegawa B. Determination of the attenuation map in emission tomography. *J Nucl Med* 2003; 44:291-315.
- Holly TA, Abbott BG, Mallah MA, Calnon DA, Cohen MC, DiFilippo. ASNC imaging guidelines for nuclear cardiology procedures. SPECT. *J Nucl Cardiol* 2010; 588-594.
- Seo Y, Wong KH, Sun M, et al. Correction of photon attenuation and collimator response for a body-contouring SPECT/CT imaging system. *J Nucl Med* 2005; 46:868-877.
- Masood Y, Liu YH, Depuey G, et al. Clinical validation of SPECT attenuation correction using X-ray computed tomography-derived attenuation maps: multicenter clinical trial with angiographic correlation. *J Nucl Cardiol* 2005; 12:676-686.
- Chua T, Kiat H, Germano G, Maurer G, Train VK, Friedman J, Berman D. Gated technetium-99m sestamibi for simultaneous assessment of stress myocardial perfusion, postexercise regional ventricular function and myocardial viability. Correlation with echocardiography and rest thallium-201 scintigraphy. *J Am Coll Cardiol* 1994; 23:1107-1114.
- Okuda K, Nakajima K, Motomura N, Kubota M, Yamaki N, Maeda H, Matsuo S, Kinuya

- S. Attenuation correction of myocardial SPECT by scatter-photopeak window method in normal subjects. *Ann Nucl Med* 2009; 23:501-6.
10. Fricke E, Fricke H, Weise R, Kammeier A, Hagedorn R, Lotz N, Lindner O, Tschoepe D, Burchert W. Attenuation correction of myocardial SPECT perfusion images with low-dose CT: evaluation of the method by comparison with perfusion PET. *J Nucl Med* 2005; 46:736-744.
 11. Tonge CM, Manoharan M, Lawson RS, et al. Attenuation correction of myocardial SPECT studies using low resolution computed tomography images. *Nucl Med Commun* 2005; 26:231-237.
 12. Matsunari I, Böning G, Ziegler SI, Kosa I, Nekolla SG, Ficaro EP, Schwaiger M. Attenuation-corrected rest thallium-201/stress technetium 99m sestamibi myocardial SPECT in normals. *J Nucl Cardiol* 1998; 5:48-55.
 13. Savi A, Rossetti C, Gilardi MC, Landoni C, Rizzo G, Ippolito M, Garraffa G, Lucignani G. Correction measured by attenuation in tomographic heart studies with single photon emission with thallium 201. Comparison with positron- emission tomographic studies with ammonium marked with nitrogen. *Radiol Med* 1999; 98:36-42.
 14. Heller EN, DeMan P, Liu YH, Dione DP, Zupal IG, Wackers FJ, Sinusas AJ. Extracardiac activity complicates quantitative cardiac SPECT imaging using a simultaneous transmission-emission approach. *J Nucl Med* 1997; 38:1882-1890.
 15. Nakajima K, Kumita S, Ishida Y, Momose M, Hashimoto J, Morita K, et al. Creation and characterization of Japanese standards for myocardial perfusion SPECT: database from the Japanese Society of Nuclear Medicine Working Group. *Ann Nucl Med* 2007; 21:505-511.
 16. Esquerre J-P, Coca FJ, Martinez S J, Guirand RE Prone decubitus: a solution to inferior wall attenuation in thallium-201 myocardial tomography. *J Nucl Med* 1989; 30:398-401.
 17. Manglos SH, Thomas FD, Gagne GM, Hellwig BJ. Phantom study of breast tissue attenuation in myocardial imaging. *J Nucl Med* 1993; 34:992-996.
 18. Biedermann M, Althoefer C, Btill U. Schw~ichtungseffekte bei der 99mTc-MIBI Belastungsmiokard 360 ° SPECT: Vergleich von Rficken- und Bauchlage. *Nucl Med* 1994; 33:8-14.